

# Entropy Measure of Stepwise Component in GPS Time Series

A. A. Lyubushin<sup>a</sup> and P. V. Yakovlev<sup>b</sup>

<sup>a</sup>*Schmidt Institute of Physics of the Earth, Russian Academy of Sciences, ul. Bol'shaya Gruzinskaya 10, Moscow, 123995 Russia  
e-mail: lyubushin@yandex.ru*

<sup>b</sup>*Ordzhonikidze Russian State Geological Prospecting University, ul. Miklukho-Maklaya 23, Moscow, 117997 Russia  
e-mail: payulyakovlev@gmail.com*

Received February 2, 2015

**Abstract**—A new method for estimating the stepwise component in the time series is suggested. The method is based on the application of a pseudo-derivative. The advantage of this method lies in the simplicity of its practical implementation compared to the more common methods for identifying the peculiarities in the time series against the noise. The need for automatic detection of the jumps in the noised signal and for introducing a quantitative measure of a stepwise behavior of the signal arises in the problems of the GPS time series analysis. The interest in the jumps in the mean level of the GPS signal is associated with the fact that they may reflect the typical earthquakes or the so-called silent earthquakes. In this paper, we offer the criteria for quantifying the degree of the stepwise behavior of the noised time series. These criteria are based on calculating the entropy for the auxiliary series of averaged stepwise approximations, which are constructed with the use of pseudo-derivatives.

DOI: 10.1134/S106935131506004X

## INTRODUCTION

In the time series analysis, it is frequently required to identify peculiar features in signal behavior such as outliers, kinks in the trend, or jump-like changes (steps) in the mean value. Identification of these peculiarities can pursue different goals. Most frequently, these features are treated as the manifestations of the malfunction of the acquisition systems or as a response to the external impacts which have nothing in common with the nature of the studied data. In other words, identification of these peculiarities in the time series is aimed at filtering them out and passing to the analysis of the “pure” data. The other problem is antithetical to the first one: these peculiarities can be considered as the signs of important changes in the nature of the data, i.e., as events that alter the behavior of the time series. In this paper, the emphasis is placed on identifying the jumps (steps) in the mean level of the signal and introducing a certain norm which describes the degree of the stepwise behavior of the time series. This is due to the fact that the suggested method is primarily intended for analyzing the GPS time series in which a part of the jumps are caused by the post-seismic effects of the earthquakes and, presumably, by the hidden events such as silent earthquakes (Dragert et al., 2001; Eberhart-Philips et al., 2003; Ito et al., 2006; Linde et al., 1996).

A broad range of the algorithms has been developed so far for identifying the characteristic elements in the behavior of the time series. In (Gvishiani et al., 2010; Soloviev et al., 2012), the apparatus of fuzzy logic is applied for morphostructural analysis of the signals.

The methods for detecting statistically significant stepwise changes in the mean value of the GPS time series are presented in (Perfetti, 2006; Riley, 2008; Borghi et al., 2012; Gazeaux et al., 2013; Gouadarzi et al., 2013; Bruni et al., 2014). The problem of revealing abrupt changes in the mean level of a signal is also topical in the analysis of the climate time series (Zurbenko et al., 1996; Ducre-Robitaille et al., 2003; Rodionov and Overland, 2005; Rodionov, 2006).

The method addressed in this paper is extremely simple for practical implementation. Besides, in fact, it uses only two parameters—the minimal and maximal bases for calculating the pseudo-derivative when averaging the stepwise approximations. Therefore, in our opinion, this method is quite competitive with the other methods previously suggested for similar purposes. The present study, in a sense, continues the paper (Lyubushin and Yakovlev, 2014) by further developing the analysis methods for the irregular noise component in the GPS time series.

## DEFINITION OF PSEUDO-DERIVATIVE

The notion of a pseudo-derivative for identifying the jumps in the time series was proposed by P.V. Yakovlev. Below, the analysis of the time series is conducted in the moving window which, in turn, is subdivided into two identical subwindows,  $L$  (left) and  $R$  (right). As a final product, the analysis should yield the function which reflects the degree of variability in the initial data.

We consider the time series  $X(t)$ ,  $t = 1, \dots, N$  in a moving window with length  $M$ . Then, the subwindows

$L$  and  $R$  have the lengths of  $[M/2]$  and  $M - [M/2]$  readings. Thus, we may compile a certain descriptive statistics of the series  $X(t)$  by considering the following quantities:

$$L_{\max}^i = \max_{i \leq t < i + [M/2]} X(t), \quad L_{\min}^i = \min_{i \leq t < i + [M/2]} X(t), \quad (1)$$

$$R_{\max}^i = \max_{i + [M/2] \leq t < i + M} X(t), \quad R_{\min}^i = \min_{i + [M/2] \leq t < i + M} X(t), \quad (2)$$

where  $i = 1, \dots, N - M$ .

We introduce two quantities

$$\Delta ED_i = R_{\max}^i - L_{\min}^i, \quad \Delta ID_i = R_{\min}^i - L_{\max}^i, \quad (3)$$

and call them the *apparent increment* and *hidden increment*, respectively.

*Pseudo-derivative on the base  $M$*  is the value

$$D_i = \frac{\Delta ED_i + \Delta ID_i}{2}, \quad (4)$$

which will be a measure of signal variability. Coefficient  $1/2$  prevents an event from being taken into account twice.

#### SIMILARITIES BETWEEN A PSEUDO-DERIVATIVE AND A DERIVATIVE

The term ‘‘pseudo-derivative’’ for quantity (4) was selected by the following reasons. Let us consider three probable cases. Since the calculations presented below are applicable for each window, index  $i$  is omitted.

(1) Let  $D > 0$ . Then,  $(R_{\max} - L_{\min})/2 > (L_{\max} - R_{\min})/2$ . Hence,  $(R_{\max} + R_{\min})/2 > (L_{\max} + L_{\min})/2$ , i.e., the center of window  $R$  is located above the center of window  $L$ . This indicates a growth of the signal.

(2) Let  $D < 0$ . Then,  $(R_{\max} - L_{\min})/2 < (L_{\max} - R_{\min})/2$ , Hence,  $(R_{\max} + R_{\min})/2 < (L_{\max} + L_{\min})/2$ , i.e., the center of window  $L$  is located above the center of window  $R$ , which indicates a decline in the signal. This case fully mirrors the previous case: the hidden and apparent increments exchange their places.

(3) Let  $D = 0$ . Then,  $(R_{\max} - L_{\min})/2 = (L_{\max} - R_{\min})/2$  or  $(R_{\max} + R_{\min})/2 = (L_{\min} + L_{\min})/2$ ; i.e., the centers of windows  $L$  and  $R$  coincide.

Thus, the direction of the increasing or decreasing trend in the signal can be determined by examining the relative positions of the centers of neighboring windows whose bottom and top boundaries correspond to the maximal and minimal values of the signal in the window, respectively. The sign of (4), just as the sign of the conventional derivative, indicates an increase or

decrease in the signal values. The same approach is applicable for finding the points of the extrema of the signal. Clearly, the value of  $D_i$  itself approximates the amplitude of the signal increment along the direction of its changes. We recall that  $i = 1, \dots, N - M$ ; i.e., each calculated value is assigned to the beginning of window  $R$  and all the values are shifted by  $[M/2]$  along the abscissa axis.

In the special case when the length  $M$  of the moving window is 2 and the signal discretization step is 1, the value of  $D_i$  fully coincides with the values of finite differences which are used for the approximation of the derivative since  $R_{\max}^i = R_{\min}^i = R$  and  $L_{\max}^i = L_{\min}^i = L$ ; hence,

$$\begin{aligned} D_i &= \frac{\Delta ED_i + \Delta ID_i}{2} = \frac{R_{\max}^i - L_{\min}^i + R_{\min}^i - L_{\max}^i}{2} \\ &= \frac{2R - 2L}{2} = R - L = X(i + 1) - X(i). \end{aligned}$$

#### CONSTRUCTING THE STEPWISE APPROXIMATION

The stepwise approximation (SA) is an instrument which is used in the time series analysis for detecting abrupt changes in the mean level of the signal against the noise.

The algorithm for constructing SA with the use of pseudo-derivative includes the following stages:

(1) calculating the pseudo-derivative of the initial signal;

(2) eliminating the moving average from the pseudo-derivative in the window with the radius equal to the base of the pseudo-derivative;

(3) finding the zeros of the obtained time series and constructing the ‘‘steps’’ in the intervals between them, where each step is the median value of the initial signal in the intervals between the zeros of the pseudo-derivative.

Let us consider stages 1 to 3 more closely. The main goal of the discussed algorithm is finding the zeros of the pseudo-derivative since, just as the zeros of a derivative, the zeros of the pseudo-derivative mark the points of the extrema of the signal; i.e., the points where the function changes its behavior (decreases or increases). If the signal contains a trend and the signal oscillations relative to this trend are small, the pseudo-derivative may not intersect the abscissa axis at all. Therefore, an implicit detrending process is required to eliminate the trends by subtracting the moving average from the values of the pseudo-derivative.

After eliminating the moving average and finding the zeros of the resulting signal, we can specify the steps by the median values of the signal in the intervals between the zeros. Since we are dealing with discrete

time, the zeros of a signal should be understood as the centers of two neighboring readings that have different signs. As a result, we obtain the SA of the initial signal. We note that the pseudo-derivative contains  $M$  fewer readings than the initial signal. Therefore, we set the first  $\left\lfloor \frac{M}{2} \right\rfloor$  readings equal to the first value of the pseudo-derivative, and the last  $M - \left\lfloor \frac{M}{2} \right\rfloor$  readings, equal to the last value. We denote the SA of the time series constructed in the way described below by  $S_M(t)$ , where  $t = 1, \dots, N$  is the integer-valued time index and  $N$  is the length of the time series in terms of the number of readings.

The size  $M$  of the window controls the number of the approximating steps. With a lower  $M$ , the SA of the signal will be more detailed. At the same time, not all the jumps of SA are of interest but only those which correspond to the maximal amplitude of the jump. However, it should be taken into account that, with the given base of calculation of the pseudo-derivative, the amplitudes of the jumps in SA are sensitive to the noise, and a part of the high-amplitude jumps is caused by the noise. Due to this, in order to suppress the noise, we use the average value of a large number of the SAs constructed for the set of the bases  $M$ , because at a point of discontinuity in the signal, SA will have a break for most of the values of  $M$ .

For this purpose, we introduce two parameters, the minimal ( $M_{\min}$ ) and maximal ( $M_{\max}$ ) bases  $M$  for calculating the pseudo-derivative. We calculate signal  $\bar{S}(t)$  as the average of all SAs:

$$\bar{S}(t) = \sum_{M=M_{\min}}^{M=M_{\max}} S_M(t) / (M_{\max} - M_{\min} + 1). \quad (5)$$

Let  $R(t)$  be the absolute increment of the averaged SA in the time window of radius  $M_{\min}/2$  with the central point  $t$ :

$$R(t) = \max_{l-M_{\min}/2 \leq q \leq l+M_{\min}/2} \bar{S}(q) - \min_{l-M_{\min}/2 \leq q \leq l+M_{\min}/2} \bar{S}(q). \quad (6)$$

From the physical sense of  $R(t)$  it follows that the maxima of  $R(t)$  fall at the jumps in the time series. We note that quantity (6) is defined for  $M_{\min}/2 + 1 \leq t \leq N - M_{\min}/2$ .

Let us formulate the quantitative criterion of the presence of a significant stepwise component in the noised time series. Hereinafter, we use the following parameters of the method:  $M_{\min} = 5$  and  $M_{\max} = 200$ . The variations in the auxiliary time series (6) contain the information about the presence of the significant jumps of the average level in the initial time series.

For identifying the significant jumps, we consider the quantity

$$R^+(t) = \max(0, R(t) - 3R_{\text{med}}), \quad (7)$$

where  $R_{\text{med}}$  is the median of (6); i.e., quantities (7) are the elevations above the level of the three median values. Then we introduce the normalized entropy of these elevations:

$$En = -\sum_t^{(+)} p(t) \log(p(t)) / \log N^+, \quad (8)$$

where symbol  $\sum_t^{(+)}$  denotes summation only by the time indices  $t$  for which  $R^+(t) > 0$ ,  $N^+$  is the total number of such indices, and  $p(t) = R^+(t) / \sum_q^{(+)} R^+(q)$  are the quantities (7) converted to the probabilities. By construction, quantity (8) satisfies the constraint  $0 \leq En \leq 1$ , and the closer it is to 1, the more chaotic the variations of quantity (7) are. The time series which is free of significant jumps is characterized by the chaotic changes of (7). Consequently, the normalized entropy for this time series is higher than for the time series containing the jumps.

## EXAMPLES OF DATA ANALYSIS

Below, the proposed method is illustrated by analyzing the daily time series of vertical displacements at different GPS sites of the IGS system. The data are freely accessible at [http://gf9.ucs.indiana.edu/daily\\_rdahmmexec/daily/](http://gf9.ucs.indiana.edu/daily_rdahmmexec/daily/).

Figures 2a and 2b show the graphs of the pseudo-derivative for the daily time series of the vertical displacements at the J568 station (37.32° N, 139.02° E) and its SA for the base  $M = 100$ . Figure 2c shows the graph of the statistics (6), which contains a significant maximum corresponding to the jump in the mean level of the averaged SA in Fig. 2d. This example illustrates the noise suppression by averaging the SAs for the different bases in formula (5): this averaging removes many of the jumps on SAs in Fig. 2b and only retains one jump, which is present in all the SAs calculated for the different bases. In this example,  $En = 0.8922$ .

In the next example, we compare the results of the analysis for two signals. One signal is the realization of the Gaussian white noise with unit variance. Its length is 20000 readings, and the jumps in the average signal level are absent. The second time series is noised and contains a stepwise component. This time series is represented by the sum  $T(t) + \varepsilon(t)$ ,  $t = 1, \dots, 2000$ , where  $\varepsilon(t)$  is the Gaussian white noise with unit variance and  $T(t)$  is a stepwise function which is zero at  $t \in [1, 250]$ ,  $[751, 1250]$ ,  $[1751, 2000]$  and 2 at  $t \in [251, 750]$ ,  $[1251, 1750]$ . The results of the analysis for these two signals are shown in Fig. 3. Comparing the values indicated in the figure captions, we can see that the normalized entropy  $En$ , which is a measure of randomness (chaos) in  $R(t)$ , has dropped from 0.9046 to

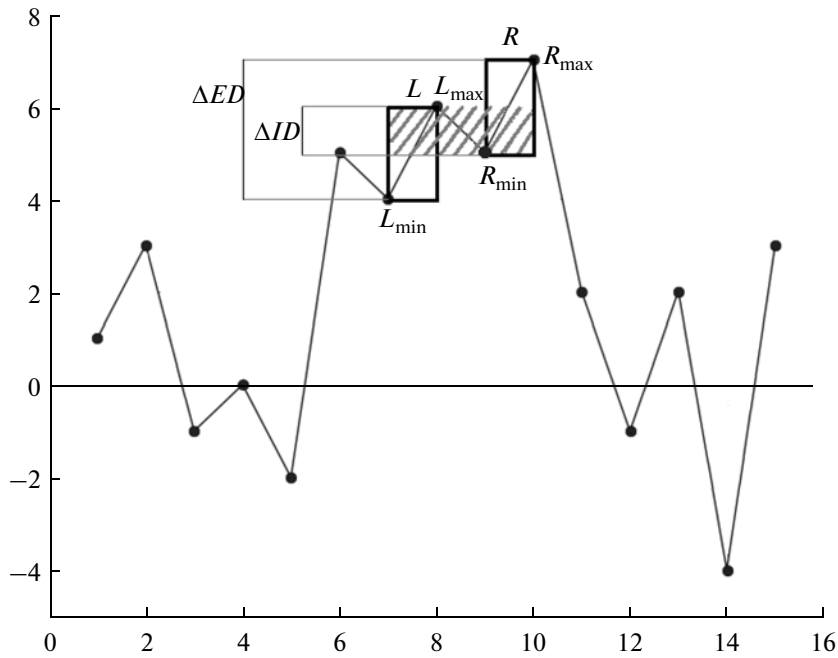


Fig. 1. The apparent and hidden increments,  $M = 4$ . The explanations are presented in the text.

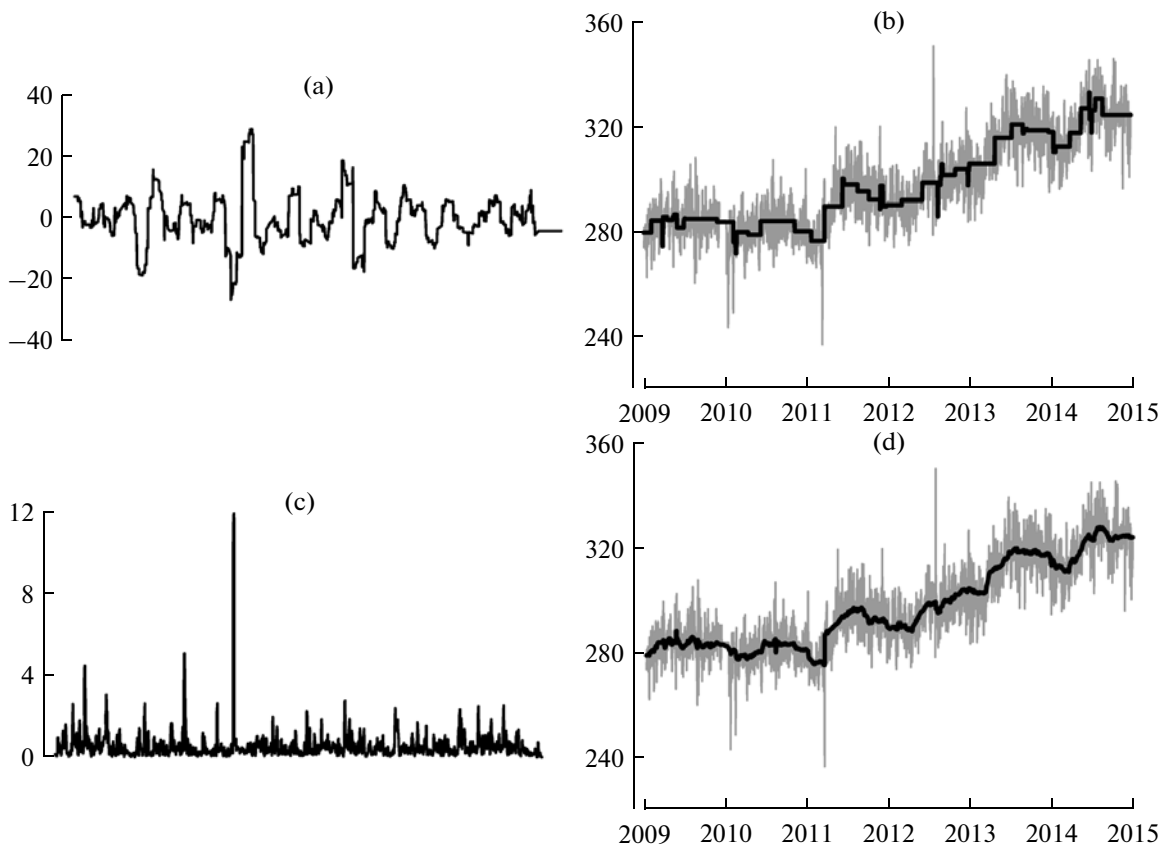
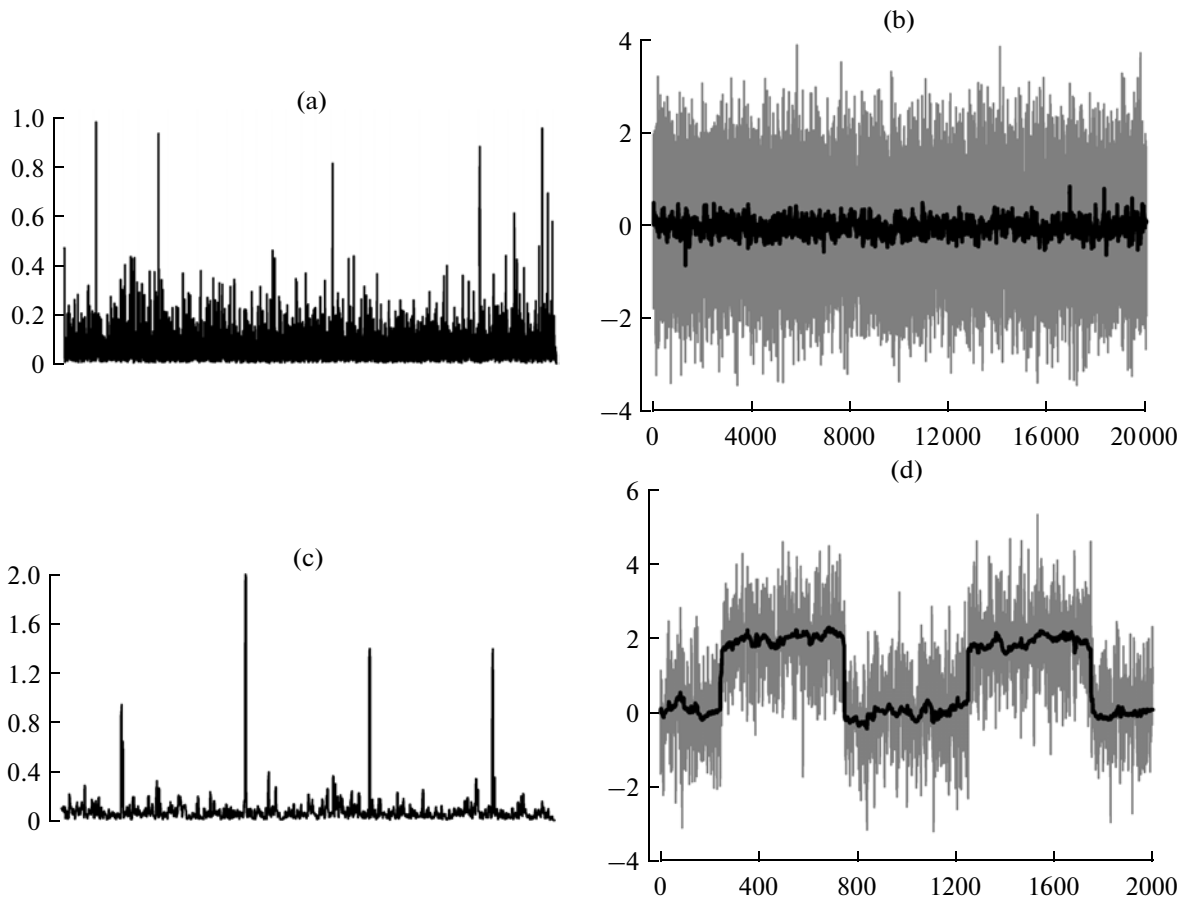


Fig. 2. (a), The pseudo-derivative of daily time series of vertical displacements at the J568 station calculated with a base of 100 readings; (b), the initial GPS signal (the gray line) and SA for the base  $M = 100$  (the thick black line); (c), the graph of the statistics  $R(t)$  according to formula (8); (d), the initial GPS signal (the gray line) and averaged SA according to formula (5) (the thick black line).  $En = 0.8373$ .



**Fig. 3.** (a), The graph of  $R(t)$ , formula (6), for the realization of the Gaussian white noise; (b), the initial time series (the gray line) and its averaged SA (the thick black line),  $En = 0.9046$ ; (c), the graph of  $R(t)$  for the artificial signal with four jumps of the mean level; (d), the initial GPS signal (the gray line) and averaged SA according to formula (5) (the thick black line).  $En = 0.7860$ .

0.7860. Besides, Fig. 3c evidently offers the decision rule for determining the time instants of the jumps: these jumps can be found by the points of the significant maxima in the statistics (6).

Figure 4 illustrates the results of analyzing two time series with lengths of 18 years for the stations ALBH (48.39° N, 123.49° W) and DELF (4.38° N, 51.99° E). We selected this pair of the time series due to their high normalized entropy which highly probably suggested the absence of the jumps in the average signal level. Indeed, their absence is proved by Figs. 4b and 4d. Figure 5 displays the results of the analysis for the time series from stations FARB (37.70° N, 123.00° E) and METS (24.40° N, 60.22° E), which contain distinctly pronounced jumps. Due to their presence, the normalized entropy for these time series is lower than for the time series in Fig. 4.

Thus, using the entropy measure (7), we can construct an automated method for exploring the time series for the presence of a stepwise component. This automated algorithm is highly valuable for analyzing the database of the GPS time series. For instance, the database used in this paper contains as of now the

three-component time series from 10590 permanent GPS stations all over the world.

For constructing this method, a natural idea is to specify the threshold value of the normalized entropy  $En^*$  which would formally separate the time series containing a stepwise component ( $En < En^*$ ) from the time series without this component ( $En \geq En^*$ ). Evidently, this boundary should be diffuse; i.e., there is a certain interval of entropy values for which the existence of low-amplitude jumps is barely detectable against the background noise. By visually analyzing the set of 40 time series, we suggest formalizing this diffuse boundary in the following way: if  $En > 0.90$ , the time series are free of jumps, and at  $En < 0.88$ , the jumps are present, i.e.,  $En^* \approx 0.89$ . The histogram of the normalized entropy is presented in Fig. 6, which provides an idea of the interval of the probable values of  $En$ .

The GPS time series frequently contain the jumps with small amplitudes which are commensurate to the amplitudes of noise variations. It is just the presence of these jumps that precludes from establishing a strict

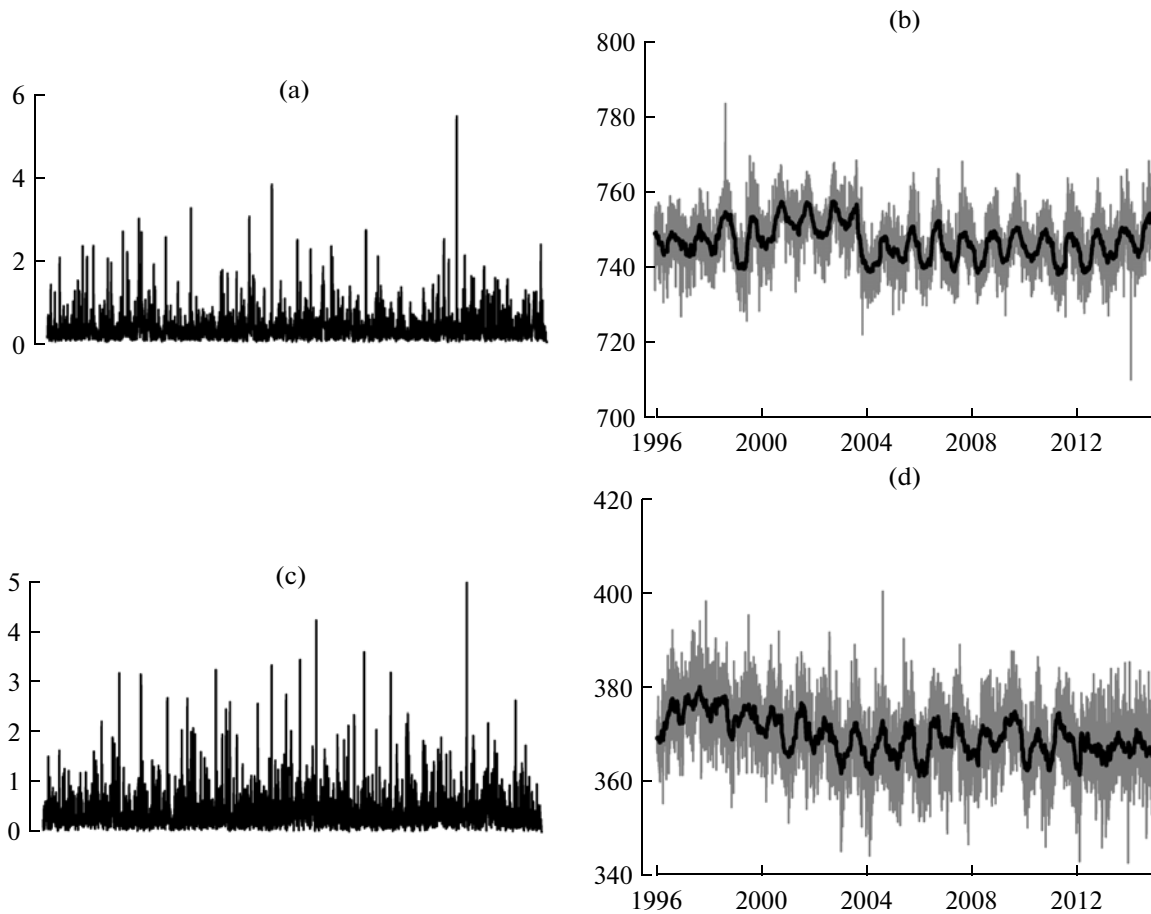


**Fig. 4.** (a), The graph of  $R(t)$  for the daily time series of vertical displacements at the ALBH station; (b), the initial GPS signal for ALBH (the gray line) and its averaged SA (the thick black line),  $En = 0.9163$ ; (c), the graph of  $R(t)$  for the daily time series of vertical displacements at the DELF station; (d), the initial GPS signal for DELF (the gray line) and its averaged SA (the thick black line).  $En = 0.9090$ .

boundary  $En^*$ . Therefore, the next idea is to directly use the quantity  $En$  as sort of a measure of non-stationarity in the behavior of the time series, which is based on estimating the stepwise component in the signal.

The results of implementing this idea are illustrated by Figs. 7 and 8. Figure 7a shows the positions of 2176 GPS stations in the western U.S., for which the daily time series are available. Below we only analyze the vertical components and use the time windows with a length of  $\sim 730$  days and a mutual shift by 7 days. At each station, we only considered the windows for which there were at most 30 missed values. The missed values were padded by the constants determined as half of the average values of the time series to the left and to the right of the missed interval on the intervals of the same length as the length of the gap. This constraint singled out the operable stations for each window. The graph showing the number of these stations as a function of the position of the time mark corresponding to the right end of the window is presented in Fig. 7b. For each time window and for each station

which was operable in a given window, we calculated the normalized entropy  $En$  by formula (8).

The rectangular area in Fig. 7a was covered by a regular  $50 \times 50$  grid. In each time window for each grid node, ten workable stations closest to the node were determined. Each node was assigned the median value calculated from the  $En$  values at these closest ten stations. Using the set of the  $En$  values at each grid node, we can construct the individual map of the spatial distribution of  $En$  which corresponds to each time window. Averaging these individual maps gives the mean map corresponding to the position of the time windows between the given dates.

Figure 7c shows the graph of the variations in the mean  $En$  calculated at all grid nodes of each individual map as a function of the time mark of the right end of the window. In the figures shown, we specified the boundaries of averaging at 2009 to 2014. By choosing these boundaries, we intended to maximally fully eliminate the influence of the number of the operable stations on the results of averaging because since 2009,

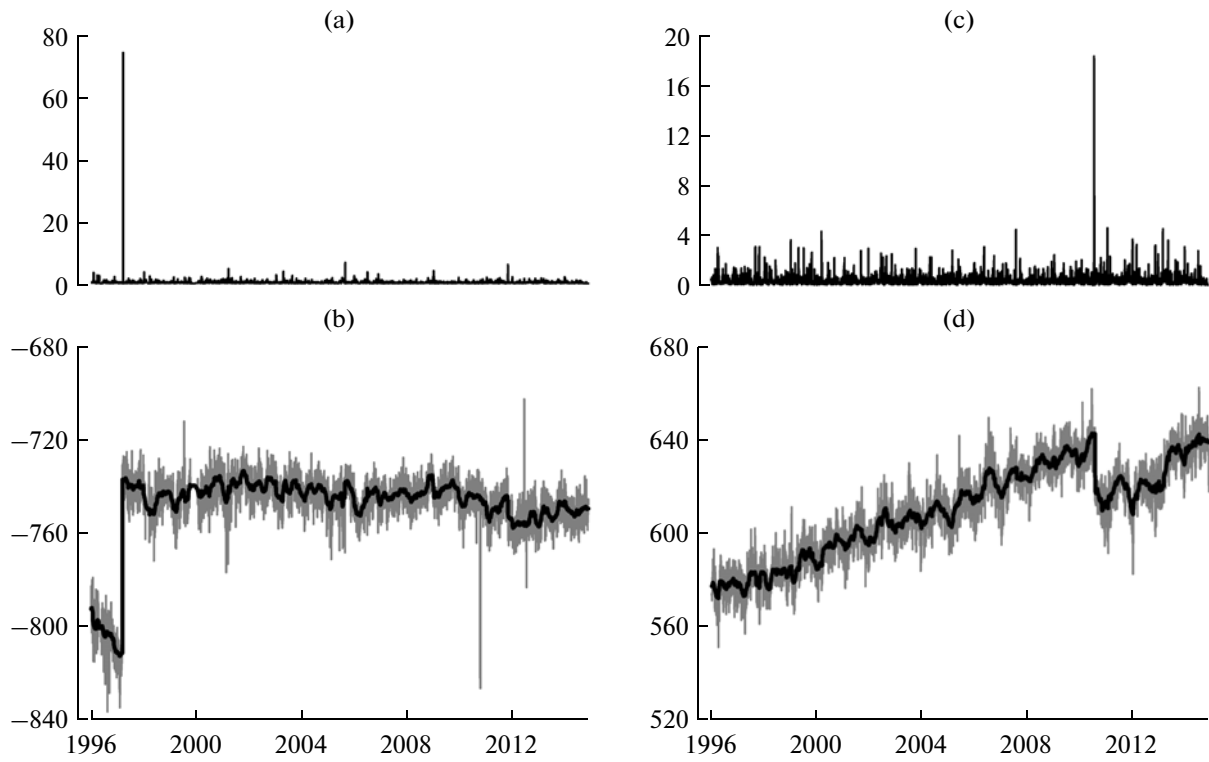


**Fig. 5.** (a), The graph of  $R(t)$  for the daily time series of vertical displacements at the FARB station; (b), the initial GPS signal for FARB (the gray line) and its averaged SA (the thick black line),  $En = 0.7090$ ; (c), the graph of  $R(t)$  for the daily time series of vertical displacements at the METS station; (d), the initial GPS signal for METS (the gray line) and its averaged SA (the thick black line).  $En = 0.8788$ .

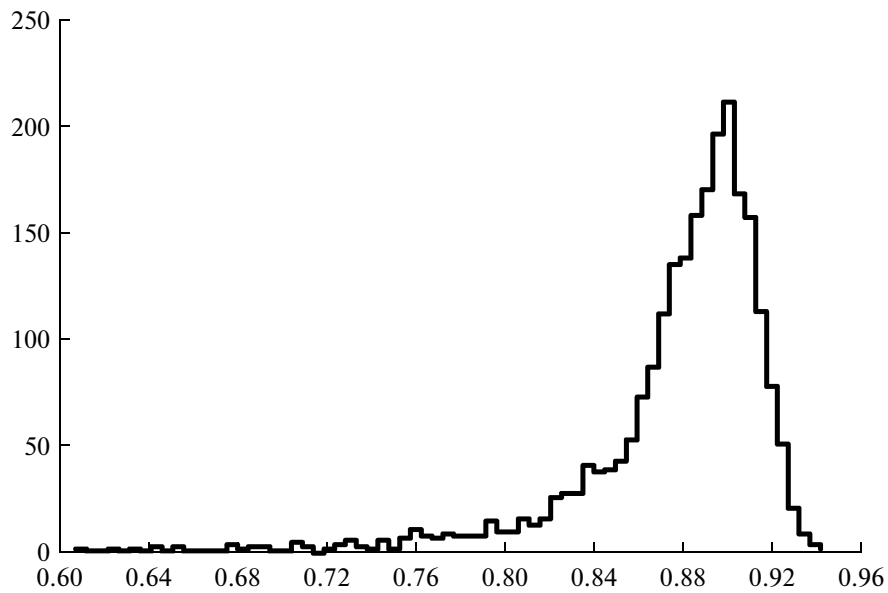


**Fig. 6.** The histogram of the normalized entropy  $En$  of 2457 daily time series of the vertical GPS displacements with a duration of at least 2000 days.

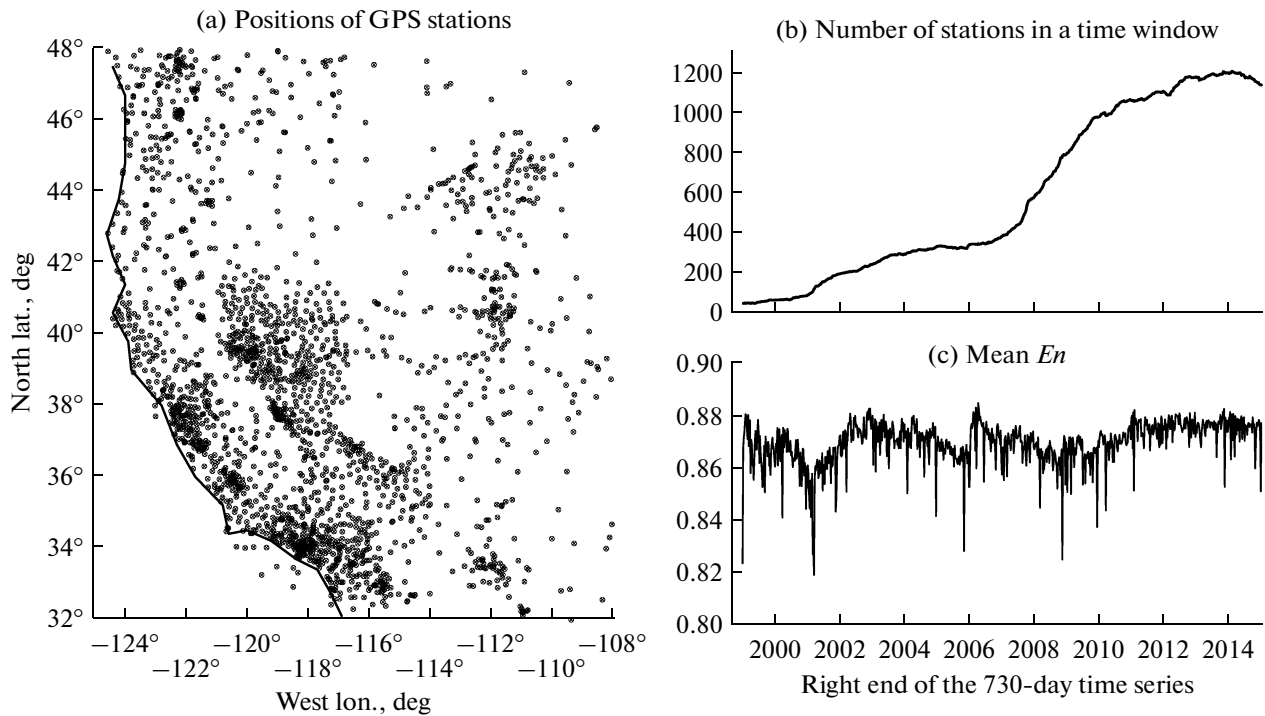


**Fig. 7.** (a), The positions of 2176 GPS stations in the western U.S.; (b), the number of the workable stations in the time window with a length of 730 days (the number of the gaps is at most 30); (c), the mean normalized entropy  $En$ , obtained by averaging the values at each point in a current time window.

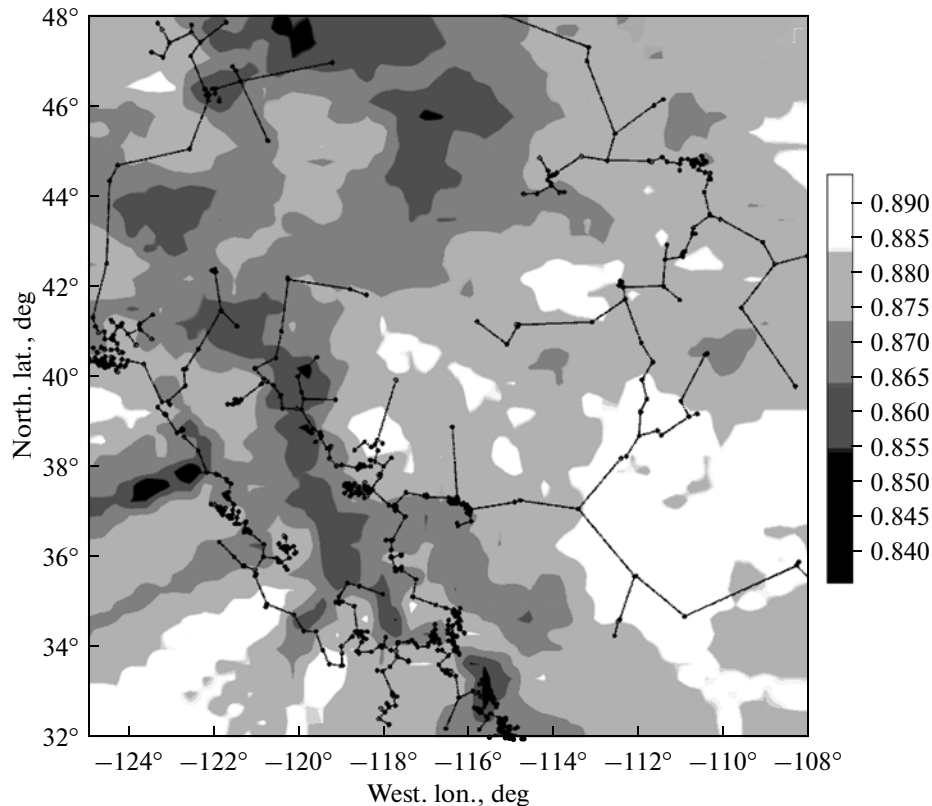


**Fig. 8.** The map of the spatial distribution of normalized entropy  $En$  obtained by averaging the maps from all the time windows with a length of 730 days and time shift of 7 days within the time interval from 2009 to 2014 (the time marks of the windows in Figs. 7b and 7c since 2011). The minimum spanning tree for the epicenters of the earthquakes of 1973–2014 with  $M \geq 4.5$  is shown.



there have been more than 1000 such stations (Fig. 7b, the time mark of the window starting from 2011). Besides, it can be seen in Fig. 7c that the average value at the grid nodes for this time interval has become noticeably stabilized.

Figure 8 shows the  $En$  map averaged over the interval of 2009 to 2014. Here, a linear area of the enhanced stepwise behavior (low  $En$ ) is observed parallel to the Pacific coast. The minimum spanning tree (Duda and Hart, 1973) for the positions of the earthquake epicenters with  $M \geq 4.5$  for 1973–2014 is shown in Fig. 8. It can be seen here that the region of low  $En$  does not fully coincide with the active seismic zones. This suggests that the presence of the jumps in the GPS time series not only reflects the postseismic effects but is also caused by the other processes such as the enhancement of the creep and the slow earthquakes.

### CONCLUSIONS

A new approach in signal analysis which uses a pseudo-derivative as a characteristic of signal variability is described. The notion of pseudo-derivative has something in common with the classical definition of the derivative. The criterion is proposed for estimating the stepwise component in the GPS time series. This criterion is based on calculating the normalized entropy of the absolute values of increments of the averaged stepwise approximation constructed with the use of a pseudo-derivative. The algorithm is developed for constructing the spatial maps reflecting the variability in the entropy criterion of the stepwise behavior of the signal. This criterion can be used for identifying the regions which are most likely to accommodate hidden geodynamic processes such as silent earthquakes.

### ACKNOWLEDGMENTS

The work was supported by the Russian Foundation for Basic Research (grant no. 15-05-00414) and Russian Federation Ministry of Science and Education (in accordance to the State Contract no. 14.577.21.0109).

### REFERENCES

- Borghini, A., Cannizzaro, L., and Vitti, A., Advanced techniques for discontinuity detection in GNSS coordinate time-series. An Italian case study, in *Geodesy for Planet Earth*, vol. 136 of *International Association of Geodesy Symposia*, Kenyon, S. et al., Eds., Berlin: Springer, 2012, pp. 627–634.
- Bruni, S., Zerbini, S., Raicich, F., Errico, M., and Santi, E., Detecting discontinuities in GNSS coordinate time series with STARS: case study, the Bologna and Medicina GPS sites, *J. Geod.*, 2014, vol. 88, no. 12, pp. 1203–1214.
- Dragert, H., Wang, K., and James, T.S., A silent slip event on the deeper Cascadia subduction interface, *Science*, 2001, vol. 292, no. 5521, pp. 1525–1528.
- Ducre-Robitaille, J.F., Vincent, L.A., and Boulet, G., Comparison of techniques for detection of discontinuities in temperature series, *Int. J. Climatol.*, 2003, vol. 23, no. 9, pp. 1087–1101.
- Duda, R.O. and Hart, P.E., *Pattern Classification and Scene Analysis*, New York: Wiley, 1973.
- Eberhart-Philips D. et al., The 2002 Denali fault earthquake, Alaska: a large-magnitude, slip-partitioned event, *Science*, 2003, vol. 300, pp. 1113–1118.
- Gazeaux, J., et al., Detecting offsets in GPS time series: first results from the detection of offsets in GPS experiment, *J. Geophys. Res. Solid Earth*, 2013, vol. 118, pp. 2397–2407.
- Goudarzi, M.A., Cocard, M., Santerre, R., and Woldai, T., GPS interactive time series analysis software, *GPS Solutions*, 2013, vol. 17, no. 4, pp. 595–603.
- Gvishiani, A.D., Agayan, S.M., Bogoutdinov, Sh.R., and Solovyov, A.A., Discrete mathematical analysis and applications in geology and geophysics, *Vestnik KRAUNTs, Nauki Zemle*, 2010, vol. 16, no. 2, pp. 109–125.
- Ito, Y., Obara, K., Shiomi, K., Sekine, S., and Hirose, H., Slow earthquakes coincident with episodic tremors and slow slip events, *Science*, 2006, vol. 26, pp. 503–506.
- Linde, A.T., Gladwin, M.T., Johnston, M.J.S., Gwyther, R.L., and Bilham, R.G., A slow earthquake sequence on the San Andreas fault, *Nature*, 1996, vol. 383, pp. 65–68.
- Lyubushin, A. and Yakovlev, P., *Properties of GPS noise at Japan islands before and after Tohoku mega-earthquake*, *SpringerPlus, Earth and Environmental Sciences*, 2014, vol. 3, pp. 364–371. <http://www.springerplus.com/content/3/1/364>. doi 10.1186/2193-1801-3-364
- Perfetti, N., Detection of station coordinate discontinuities within the Italian GPS Fiducial Network, *J. Geod.*, 2006, vol. 80, pp. 381–396.
- Riley, W.J., Algorithms for frequency jump detection, *Metrologia*, 2008, vol. 45, pp. 154–161.
- Rodionov, S. and Overland, J.E., Application of a sequential regime shift detection method to the Bering Sea ecosystem, *ICES J. Mar. Sci.*, 2005, vol. 62, pp. 328–332.
- Rodionov, S.N., Use of prewhitening in climate regime shift detection, *Geophys. Res. Lett.*, 2006, vol. 33, L12707.
- Soloviev, A.A., Agayan, S.M., Gvishiani, A.D., Bogoutdinov, Sh.R., and Chulliat, A., Recognition of disturbances with specified morphology in time series: Part 2. Spikes on 1-s magnetograms, *Izv., Phys. Solid Earth*, 2012, vol. 48, no. 5, pp. 395–409.
- Zurbenko, I., Porter, P.S., Gui, R., Rao, S.T., Ku, J.Y., and Eskridge, R.E., Detecting discontinuities in time series of upper-air data: development and demonstration of an adaptive filter technique, *J. Clim.*, 1996, vol. 9, pp. 3548–3560.

Translated by M. Nazarenko